Generation and detection of coherent magnetron motion in Fourier transform ion cyclotron resonance mass spectrometry

Ruidan Chen, Shenheng Guan,[a] and Alan G. Marshall[a]
Department of Chemistry, The Ohio State University, Columbus, Ohio 43210

(Received 29 June 1993; accepted 14 October 1993)

One of the most useful recent ion cyclotron resonance (ICR) developments is the conversion of magnetron motion to cyclotron motion by azimuthal quadrupolar excitation in the presence of ion-neutral collisions. The technique offers a mass-selective means for "shrink-wrapping" an ion cloud into a tight packet along the central axis of an ICR ion trap for enhanced signal to noise ratio, mass resolving power, and other advantages. However, the process itself is not directly observable. In this paper, we show that the conversion may be rendered observable by converting coherent magnetron motion (produced by off-axis ionization during a period short compared to the magnetron frequency) to coherent cyclotron motion, followed by subsequent dipole detection at ω_+ (reduced cyclotron frequency) or quadrupolar detection at ω_c (unperturbed cyclotron frequency) and $2\omega_+$. Detection at ω_c eliminates the ICR frequency shift due to the electrostatic trapping potential, providing for increased mass accuracy; detection at $2\omega_+$ may offer increased mass resolving power. The observed signal behavior as a function of excitation amplitude–duration product is predicted theoretically and confirmed experimentally for both types of detection. Unlike the otherwise analogous 180° pulse in nuclear magnetic resonance (NMR), the magnetron-to-cyclotron interconversion may be phase-coherent with respect to both initial and final states. Finally, we show how coherent magnetron motion of two ion packets of different magnetron phase can be converted to cyclotron motion of two ion packets of different cyclotron phase, and we discuss the implications of that process.

I. INTRODUCTION

In the past decade, Fourier transform ion cyclotron resonance mass spectrometry (FT/ICR/MS) has become one of the most exciting areas in mass spectrometry, both in fundamental developments and applications.[1–22] The extraordinary analytical value of FT/ICR/MS results from its versatility and unique combination of features; (a) ultrahigh mass resolving power and mass accuracy (for unequivocal determination of ion chemical formula); (b) capability to interface with a variety of soft ionization techniques for analysis of involatile biocompounds; and (c) ion trapping for self-chemical ionization, ion-molecule reaction chemistry, photodissociation, and multistage MS^n in a single instrument.

Virtually every FT/ICR experiment is carried out with a cubic, tetragonal, or cylindrical ion trap placed in a strong static magnetic field. The two trap electrodes perpendicular to the magnetic field are usually biased to a positive (negative) voltage above ground to trap positive (negative) ions. The approximately axial quadrupolar "trapping" potential inside the trap restricts the freedom of ions to move axially away from the center of the trap along the magnetic field direction. The combined magnetic field and the electrostatic trapping potential effectively confine radial and axial ion motion. In the absence of a time-varying ("excitation") electric field, ion motion may be analyzed into three independent cyclotron rotation, magnetron rotation, and axial ("trapping") oscillation modes.[23]

Ions are normally detected in FT/ICR/MS experiments by dipolar excitation followed by dipolar detection at the reduced cyclotron frequency, ω_+ (see Sec. II). For example, ions generated by an electron beam injected along the symmetry axis of the trap form an ion "packet" with an initial diameter somewhat larger (due to Coulomb repulsions) than the electron beam diameter. Coherent cyclotron motion of the ion packet may be excited by applying a rf voltage signal (whose Fourier transform spectrum contains a component at the ion cyclotron frequency) differentially to a pair of opposed electrodes whose surfaces are parallel to the magnetic field direction. Following excitation, the coherently orbiting ion packet induces between a pair of opposed detection electrodes a differential image current that may be converted to a voltage which may be amplified, digitized, and recorded.[24,25] Coherence of cyclotron motion (i.e., all ions moving with essentially the same cyclotron phase) is essential to efficient ICR detection.[26]

Until recently, magnetron motion in an ICR ion trap has been largely ignored, except for its deleterious effects with respect to radial diffusion (see below) and signal loss due to electrical resistance in the trap electrode circuit.[27] However, one of the most important new techniques in ICR mass spectrometry is the use of quadrupolar excitation to interconvert between pure magnetron and pure cy-

[a]Current address: National High Magnetic Field Laboratory, Florida State University, 1800 East Paul Dirac Drive, Tallahassee, FL 32306-4055. (Also a member of the Department of Chemistry at Florida State University.)

 0021-9606/94/100(3)/2258/9/$6.00

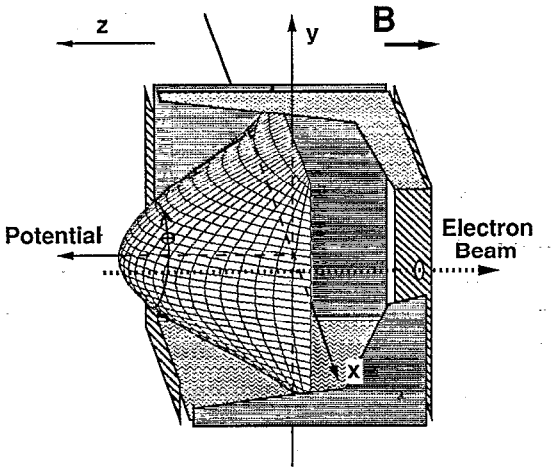

FIG. 1. Radial component of the electrostatic trapping potential in the xy midplane ($z=0$) of a cubic ICR ion trap. An electron beam travels along an off-axis line ($x=x_0$, $y=0$) parallel to the trap symmetry axis ($x=0$, $y=0$). Immediately after their formation, ions have a finite magnetron radius and the ions precess in a magnetron orbit (dark curve) along an isopotential contour.

clotron motion. Initially demonstrated for single-frequency experiments in a Penning ion trap,[28,29] the technique has been extended to broad band FT/ICR experiments in a cubic ion trap.[30] In the presence of ion-neutral collisions, ions are cooled and axialized to form a compact ion packet at the center of the ICR ion trap, leading to the following advantages: (a) improved ICR peak shape and detection sensitivity (factor of 100 in some cases);[31] (b) improved mass resolving power (up to factor of 500);[31] (c) improved ion remeasurement efficiency (up to 99%) for additional increase in signal to noise ratio and/or multiple experiments with a single trapped-ion packet;[32] (d) extended trapping period to allow for thousands of ion-neutral collisions to release excess ion internal electronic or vibrational excitation energy;[30] (e) improved transfer efficiency to move ions through a narrow conductance limit;[31] and (f) reduced z-ejection from excitation at $2\omega_z$ and $\omega_+ \pm 2\omega_z$; etc.

Unfortunately, in spite of the wide-ranging impact of the quadrupolar excitation method, the process itself is usually invisible, because initially incoherent magnetron motion is converted into (unobservable) incoherent cyclotron motion. In this paper, we show that coherent magnetron motion may be generated by forming ions off-axis. Specifically, ions are generated by electron ionization along a line parallel to the magnetic field direction but radially displaced from the central symmetry z-axis of the trap. Immediately after their formation, ions thus possess a non-zero magnetron radius equal to the distance between the symmetry axis of the trap and the electron beamline. Ions then circulate at the magnetron frequency in their magnetron orbit (see Fig. 1). If the electron beam is short compared to one magnetron rotation period, then the ion initial spatial distribution is small and magnetron motion of the initial ion packet is coherent. Quadrupolar excitation may then be used to convert the magnetron coherence to a cyclotron coherence which may be observed by either dipolar or quadrupolar detection.

Coherent ion cyclotron motion may be generated by dipolar excitation of an ion packet initially at rest near the center of the trap.[22] Alternatively, some degree of magnetron coherence has been observed in laser desorption experiments as well.[33] In previous work,[34] we proved theoretically that the conversion from magnetron to cyclotron motion is formally analogous to a population inversion process in a two-level energy manifold [e.g., spin one-half nuclei in nuclear magnetic resonance (NMR)]. Here, we demonstrate experimentally that *coherent* magnetron motion can be completely converted to *coherent* cyclotron motion by azimuthal single frequency quadrupolar excitation. The experimentally observed ion response to such a conversion process is shown to agree well with theoretical predictions.

Finally, we also show how to generate two coherent spatially separated ion packets with a controllable relative magnetron phase difference. If the magnetron motion of each of those ion packets is converted to cyclotron motion, the relative magnetron phase difference is conserved as a relative cyclotron phase difference. We use the newly developed method to demonstrate experimentally the importance of cyclotron phase coherence in ICR detection. Although the formalism developed here is for a cubic ICR ion trap, extension to other trap geometry is straightforward and does not affect the qualitative conclusions of this paper.

Although the present paper deals with quadrupolar *excitation*, excitation and detection for a given ion cyclotron trap operating mode are related by the reciprocity principle of electrostatics.[35–37] Thus, some of the formal development for the cubic trap in this paper is anticipated in prior treatments of quadrupolar *detection* in a Penning trap geometry.[38–40]

II. THEORY

Here we present the minimal formal content needed to describe the present experiments. Previously published results are given without derivation. For a cubic ICR ion trap,[41] the electrostatic trapping potential, Φ_{trap}, near the center of the trap may be expressed approximately as

$$\Phi_{\text{trap}} = V_{\text{trap}}\left[\gamma - \frac{\alpha}{2a^2}(x^2+y^2-2z^2)\right] \tag{1}$$

in which V_{trap} is the dc voltage applied to each of the two opposed trapping electrodes, a is the trap edge length, and $\gamma=1/3$ and $\alpha=2.773\,73$, respectively.[42,43]

We have previously derived the azimuthal quadrupolar excitation potential for a cubic trap[22,34]

$$\Phi_{xy}(x,y,z) = \frac{3\alpha V_{xy}(t)}{2a^2}(x^2-y^2) \tag{2}$$

in which $V_{xy}(t)$ is the excitation voltage applied to the electrodes whose surfaces are parallel to the magnetic field. We found it convenient to represent the equations of motion for magnetron/cyclotron interconversion process as

$$\frac{d\mathbf{V}^+}{dt}-i\omega_+\mathbf{V}^+-i\frac{\Omega(t)}{2}\mathbf{V}^{-*}=0, \tag{3a}$$

$$\frac{d\mathbf{V}^-}{dt}-i\omega_-\mathbf{V}^-+i\frac{\Omega(t)}{2}\mathbf{V}^{+*}=0, \tag{3b}$$

$$\Omega(t)=\frac{6q\alpha V_{xy}(t)}{ma^2(\omega_+-\omega_-)}, \tag{3c}$$

in which ω_+ is the reduced cyclotron frequency, ω_- is the magnetron frequency, and $\Omega(t)$ represents a "coupling" between magnetron and cyclotron motions (see below).

$$\omega_\pm\equiv\frac{\omega_c}{2}\pm\sqrt{\frac{\omega_c^2}{4}-\frac{\omega_z^2}{2}}, \tag{4}$$

$\omega_c=qB/m$ is the unperturbed cyclotron frequency, and $\omega_z=(2\alpha qV_{\text{trap}}/ma^2)^{1/2}$ is the axial oscillation (trapping) frequency, and $\omega_-=2\alpha V_{\text{tr}}/a^2B$.

In Eq. (3), $\mathbf{V}^+$ and $\mathbf{V}^-$ are the cyclotron and magnetron velocity vectors, and the Cartesian coordinates (x,y) are represented as mathematically complex (x,iy) to render the equations more compact,

$$\mathbf{V}^+\equiv\dot{\rho}-i\omega_-\rho, \tag{5a}$$

$$\mathbf{V}^-\equiv\dot{\rho}-i\omega_+\rho. \tag{5b}$$

The concept and use of V-vectors has previously been described in detail by Brown and Gabrielse.[23] In the absence of a time-varying electric excitation field, the equation for $\mathbf{V}^+$ [Eq. (3a)] and $\mathbf{V}^-$ [Eq. (3b)] are independent and the cyclotron and magnetron motions may be treated as independent "normal modes." The (complex) position vector, $\rho=x+iy$, and its derivative, $\dot{\rho}$, may then be expressed as functions of $\mathbf{V}^+$ and $\mathbf{V}^-$

$$\rho=-\frac{i(\mathbf{V}^+-\mathbf{V}^-)}{\omega_p}, \tag{6a}$$

and

$$\dot{\rho}=\frac{\omega_+\mathbf{V}^+-\omega_-\mathbf{V}^-}{\omega_p}, \tag{6b}$$

in which

$$\omega_p=\omega_+-\omega_-. \tag{6c}$$

A. Single-frequency azimuthal quadrupolar resonant excitation

For the present purpose, it suffices to solve the equations of ion motion for single frequency on-resonance excitation. A special transformation may be used to convert Eqs. (3) to Bloch-type magnetic resonance equations.[34] For example, complete conversion from magnetron to cyclotron motion is formally analogous to a 180° spin-flip of spin one-half nuclei. However, the individual azimuthal (transverse magnetization) phase in the Bloch equations has no physical significance for a spin-flip angle of zero or 180°, whereas either pure magnetron or pure cyclotron motion in ICR may be coherent with well-defined phase angle. We therefore require a different approach to derive solutions which retain that phase information. As suggested by Bollen *et al.*,[28] we simplify the above equation by introducing the following transform (analogous to the "rotating frame" in magnetic resonance)

$$\mathbf{V}^+=A^+(t)e^{i\omega_+t}, \tag{7a}$$

$$\mathbf{V}^-=A^-(t)e^{i\omega_-t}. \tag{7b}$$

Substituting Eqs. (7) into Eqs. (3) and noting that we shall be interested in those solutions corresponding to single-frequency on-resonance quadrupolar excitation, $\Omega(t)=\Omega_0e^{i\omega_et}$, we find

$$\frac{dA^+}{dt}-\frac{i\Omega_0}{2}A^{-*}=0, \tag{8a}$$

$$\frac{dA^-}{dt}+\frac{i\Omega_0}{2}A^{+*}=0, \tag{8b}$$

$$\Omega_0=\frac{3q\alpha V_{xy}}{ma^2\omega_p} \tag{8c}$$

in which V_{xy} is the amplitude of the excitation voltage. Ω_0 now has a simple physical interpretation, Ω_0t represents the (phase) angle for interconversion between magnetron and cyclotron modes (e.g., $\Omega_0t=0$ and π correspond to pure magnetron or pure cyclotron motion, if the system starts in pure magnetron mode). If the initial cyclotron velocity is zero, $A^+(0)=0$, and initial magnetron velocity is, $A^-(0)=A_0^-=|A_0^-|e^{i\phi-}$, one can prove that the above equations have the following solutions:

$$A^+=\frac{A_0^-}{2}(e^{i\Omega_0t/2}-e^{-i\Omega_0t/2})=iA_0^-\sin\left(\frac{\Omega_0t}{2}\right), \tag{9a}$$

$$A_-=\frac{A_0^-}{2}(e^{i\Omega_0t/2}+e^{-i\Omega_0t/2})=A_0^-\cos\left(\frac{\Omega_0t}{2}\right). \tag{9b}$$

Therefore,

$$\mathbf{V}^+=iA_0^-\sin\left(\frac{\Omega_0t}{2}\right)e^{i\omega_+t}$$

$$=|A_0^-|\sin\left(\frac{\Omega_0t}{2}\right)\exp[i(\omega_+t+\phi_-+\pi/2)], \tag{10a}$$

$$\mathbf{V}^-=A_0^-\cos\left(\frac{\Omega_0t}{2}\right)e^{i\omega_-t}$$

$$=|A_0^-|\cos\left(\frac{\Omega_0t}{2}\right)\exp[i(\omega_-t+\phi_-)] \tag{10b}$$

in which $|A_0^-|$ is the amplitude of the initial magnetron velocity; and ϕ_- is the initial phase of the magnetron velocity, $\mathbf{V}^-$. The phase, Ω_0t, in the sin or cos functions is the previously defined "flip angle,"[34] so that complete conversion (from pure magnetron to pure cyclotron motion) is first achieved when $\Omega_0t=\pi$. Importantly, Eq. (10) shows that in a single-frequency on-resonance excitation process, the phase of the initial magnetron velocity is *preserved* (after magnetron-to-cyclotron conversion) in the respective cyclotron velocity [see. Eq. 10(a)].

B. Relation between *V*-vectors and the magnetron and cyclotron radius vectors

After quadrupolar on-resonance excitation is removed, the azimuthal (radial) position vector, ρ, may be analyzed into two independent circular (magnetron and cyclotron) motions

$$\rho=\rho_+e^{i\omega_+t}+\rho_-e^{i\omega_-t} \tag{11}$$

in which ρ_+ and ρ_- are the respective radius vectors for ion cyclotron and magnetron motions. We can evaluate ρ_+ and ρ_- at the instant at which the excitation is removed. The relation between the A vectors [defined in Eqs. (7)] and the cyclotron or magnetron radius vectors may be found by substituting Eq. (11) and Eqs. (7) into Eq. (6a) to give

$$\rho_+e^{i\omega_+t}+\rho_-e^{i\omega_-t}=-\frac{i(A^+e^{i\omega_+t}-A^-e^{i\omega_-t})}{\omega_p}. \tag{12}$$

By comparing the coefficients preceding $e^{i\omega_+t}$ and $e^{i\omega_-t}$, we find

$$\rho_+=-iA^+/\omega_p, \tag{13a}$$

$$\rho_-=iA^-/\omega_p. \tag{13b}$$

C. Azimuthal dipolar and quadrupolar detection

To predict the ion response to quadrupolar excitation, we need first examine the dependence of induced image current on ion cyclotron/magnetron radius vectors in both dipolar and quadrupolar detection procedures. The ion position coordinates, x and y, may be expressed as the vector sum of the ion magnetron and cyclotron radii,

$$x=\rho_+\cos(\omega_+t)+\rho_-\cos(\omega_-t), \tag{14a}$$

$$y=\rho_+\sin(\omega_+t)+\rho_-\sin(\omega_-t). \tag{14b}$$

The corresponding velocities may be written as

$$\dot{x}=-\omega_+\rho_+\sin(\omega_+t)-\omega_-\rho_-\sin(\omega_-t), \tag{15a}$$

$$\dot{y}=\omega_+\rho_+\cos(\omega_+t)+\omega_-\rho_-\cos(\omega_-t). \tag{15b}$$

For an arbitrary detection electrode arrangement, the image current, I, induced by the azimuthal motion [Eq. (11)] may be expressed as[28]

$$I=q\mathbf{v}\cdot\mathbf{E}_i \tag{16}$$

in which $\mathbf{v}=\dot{x}\mathbf{i}+\dot{y}\mathbf{j}$ is the azimuthal velocity of the ion of charge, q, and $\mathbf{E}_i$ is the electric field generated by the electrode at unit potential from which the current is flowing and by the electrode at negative unit potential to which the current is flowing and all the other electrodes are at ground potential. To determine the dipolar detected response in a cubic ICR trap, we begin by noting that the electric field, $\mathbf{E}_{\text{dipolar}}$, near the center of the trap (produced by applying ±1 V to the two opposed detector electrodes) may be approximated as a spatially uniform field in the x-direction (i.e., pure real in our complex notation)

$$\mathbf{E}_{\text{dipolar}}=\beta/a, \tag{17}$$

in which β is the cubic trap geometric factor, 0.73; and a is the trap edge length.[37] By reciprocity,[35–37] the dipole-detected image current induced by azimuthal ion motion, is therefore obtained from Eq. (17) and the time-derivative of Eq. (14a),

$$\begin{aligned}I(t)&=(q\beta/a)[\rho_+\omega_+\sin(\omega_+t)+\rho_-\omega_-\sin(\omega_-t)]\\&=I_d(\omega_+)\sin(\omega_+t)+I_d(\omega_-)\sin(\omega_-t).\end{aligned} \tag{18}$$

Thus, conventional dipolar detection for ions of a single mass-to-charge ratio produces signals at the cyclotron frequency, ω_+, and at the magnetron frequency, ω_-, if both cyclotron and magnetron motions are coherently excited. The cyclotron dipole-detected current signal magnitude, $I_d(\omega_+)$, is proportional to the cyclotron radius and frequency and the magnetron current signal, $I_d(\omega_-)$, is proportional to the magnetron radius and frequency

$$I_d(\omega_+)=(q\beta/a)\rho_+\omega_+, \tag{19a}$$

$$I_d(\omega_-)=(q\beta/a)\rho_-\omega_-. \tag{19b}$$

Of course, in the (usual) case that the detection circuit is predominantly capacitive, the corresponding voltage signal will be frequency-independent.[24,25,40]

For azimuthal quadrupolar detection,[40] we proceed as before to determine first the electric field (in complex notation) produced by applying 1 V to each of a pair of opposed electrodes at $x=\pm a/2$ and -1 V to each of a pair of opposed electrodes orthogonal to the first pair at $y=\pm a/2$, remembering that electric field is the negative gradient of potential [Eq. (2)],

$$\mathbf{E}_{\text{quadrupolar}}=-\nabla\Phi^0_{xy}=-(3\alpha/a^2)(x-iy). \tag{20}$$

Again by reciprocity, the induced current signal for azimuthal quadrupolar detection (i.e., add the signals from electrodes at $x=\pm a/2$ and subtract the signals from electrodes at $y=\pm a/2$) is obtained from Eqs. (14)–(16) and Eq. (20) as

$$\begin{aligned}I&=\frac{3q\alpha}{a^2}[\rho_+^2\omega_+\sin(2\omega_+t)+2\rho_+\rho_-\sin(\omega_c t)\\&\quad+\rho_-^2\omega_-\sin(2\omega_-t)]\\&=I_q(2\omega_+)\sin(2\omega_+t)+I_q(\omega_c)\sin(\omega_c t)\\&\quad+I_q(\omega_-)\sin(\omega_-t).\end{aligned} \tag{21}$$

From Eq. (21), we predict that only the two peaks at frequencies $2\omega_+$ and ω_c will usually be seen in a spectrum produced by azimuthal quadrupolar detection. (Ordinarily, the signal component at frequency, $2\omega_-$, is lower in frequency than the low-frequency cutoff for the detection circuit). By analogy to Eq. (19), we have

$$I_q(2\omega_+)=(3q\alpha/a^2)\rho_+^2\omega_+, \tag{22a}$$

$$I_q(\omega_c)=(6q\alpha/a^2)\rho_+\rho_-\omega_c, \tag{22b}$$

$$I_q(2\omega_-)=(3q\alpha/a^2)\rho_-^2\omega_-. \tag{22c}$$

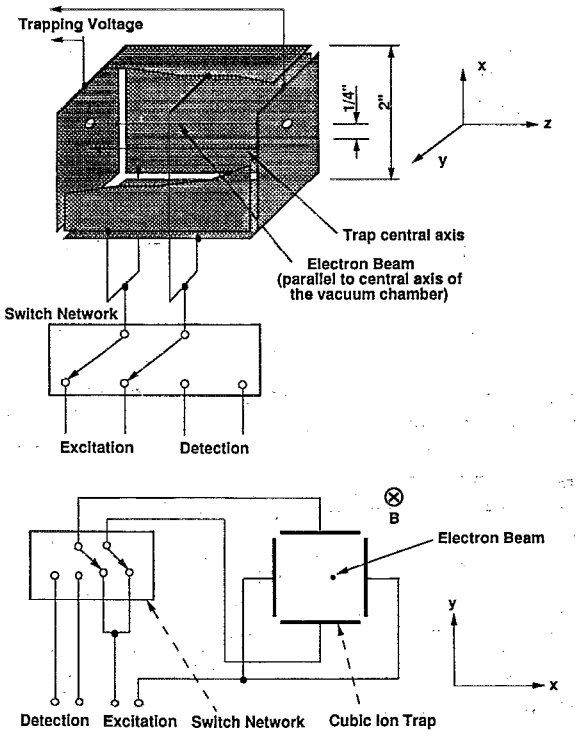

FIG. 2. Schematic representations of a cubic ICR ion trap (5.08 cm on a side) in which ions are formed by an electron beam displaced by 0.635 cm from the central axis of the trap, showing electrode connections for quadrupolar excitation/quadrupolar detection (top) and quadrupolar excitation/dipolar detection (bottom). Excitation and detection events are isolated by a switch network which is triggered during the experimental event sequence.

III. EXPERIMENT

All experiments were carried out on an Extrel FTMS-1000 spectrometer (Extrel FTMS Millipore Corp., Madison, WI) operating at 3 T. The homemade vacuum chamber is pumped with a cryopump (CryoTorr-8, Helix Technology, Waltham, MA) with a pumping speed of 2000 L/s. An ionizing electron beam passes through a 5.08 cm cubic trap parallel to the magnetic field direction, but displaced laterally by 0.635 cm from the central axis of the trap (see Fig. 2).

Benzene was admitted into the vacuum chamber through a leak valve (Model 951-5100, Varian, Palo Alto, CA). Benzene molecular ions were produced by electron impact ionization (13 eV electron beam for 1 ms at an emission current of 550–1750 μA measured on a collector located outside the more distant trap electrode) at a sample pressure of $\sim 5\times 10^{-8}$ Torr. Trapping potential was 4 V for all experiments. The magnetron frequency, $\nu_- = \omega_-/2\pi = 228$ Hz. The electron beam in such an off-center trap creates ions with a large initial magnetron radius; moreover, the ion magnetron motion is spatially coherent because the electron beam duration is short (1 ms) compared to one period of the magnetron motion ($\sim$4.4 ms).

Coherent magnetron motion is converted to coherent cyclotron motion by single-frequency resonant azimuthal quadrupolar excitation at ω_c. The experimental configuration for producing the azimuthal quadrupolar excitation potential in a cubic ICR trap has been described previously.[30] The conversion process is monitored by either azimuthal quadrupolar or conventional dipolar detection, as shown in Fig. 2. For quadrupolar excitation or quadrupolar detection, all four electrodes parallel to the magnetic field are used.[22] A homebuilt switching network isolates excitation and detection events. The same switching network is used to switch between quadrupolar excitation and dipolar detection.

IV. RESULTS AND DISCUSSION

In a typical FT/ICR experiment, ions are generated or injected along the symmetry axis (z-axis) of the trap and the initial magnetron radius (i.e., off-axis displacement of the center of the cyclotron orbit) of the ions may be neglected. If desired, coherent ion magnetron motion may be excited by resonant azimuthal dipolar excitation at the magnetron frequency, ω_-, just as coherent ion cyclotron motion may be excited by resonant dipolar excitation at ω_+. However, since the magnetron frequency is essentially mass-independent at m/z values below the "critical" mass,[12] such magnetron excitation is generally not mass-selective. Moreover, magnetron motion, even if coherent, is generally not detectable, because of the magnetron frequency (typically $\sim$100 Hz) is usually lower than the low-frequency limit of the detection circuit (typically a few kHz).

At high neutral gas pressure, ions generated along the center line of the trap collide with neutrals and gradually lose their potential energy. An important consequence of that potential energy loss is magnetron orbital radius expansion, since magnetron potential energy decreases with increasing magnetron radius.[44] In general, the collisionally-expanded magnetron orbital motion is incoherent and the distribution of ion radii is large, so that the magnetron motion is undetectable. Nevertheless, Dunbar *et al.* have observed ion magnetron motion based on a presumed initial ion distribution asymmetry which resolves into a cloud of unsymmetrically distributed charge and induces an oscillating magnetron signal on the receiver electrodes.[44] Ion magnetron motion has also been observed by Laude *et al.* in laser desorption experiments.[33]

In this work we generate ions of nonzero magnetron radius by directing an off-axis electron beam into a cubic ICR ion trap. If the electron beam duration is short compared to one cycle of the magnetron orbital motion, then the resulting ion packet is magnetron-coherent. With this approach, we are also able to produce packets of ions of different magnetron orbital phase by use of short electron beam pulses separated in time by a known fraction of one magnetron orbital period.

A. Observation of interconversion between magnetron and cyclotron motion

In our trap configuration, the magnetron/cyclotron conversion process may easily be monitored by either dipolar or quadrupolar detection as follows. Following quadrupolar excitation, the dependence of dipole-detected ion

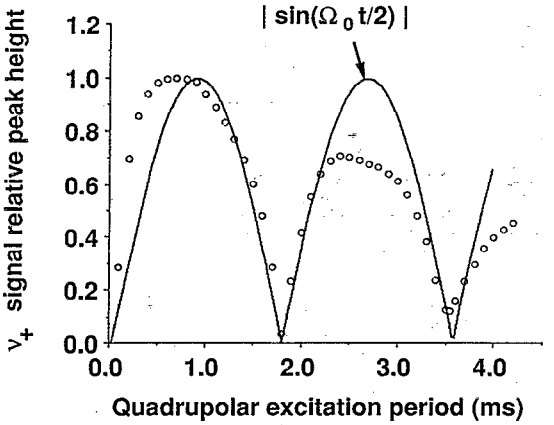

FIG. 3. Oscillation of experimental dipole-detected magnitude-mode (absolute-value mode) spectra peak height (open circles) at the cyclotron frequency, ν_+, as a function of the duration of a prior quadrupolar excitation event [12 $V_{(p\text{-}p)}$ at frequency, ν_c]. The theoretical $|\sin(\Omega_0 t/2)|$ behavior predicted by Eq. (23) is shown as the solid curve, whose maxima and zero-values correspond to pure cyclotron and pure magnetron motion, respectively.

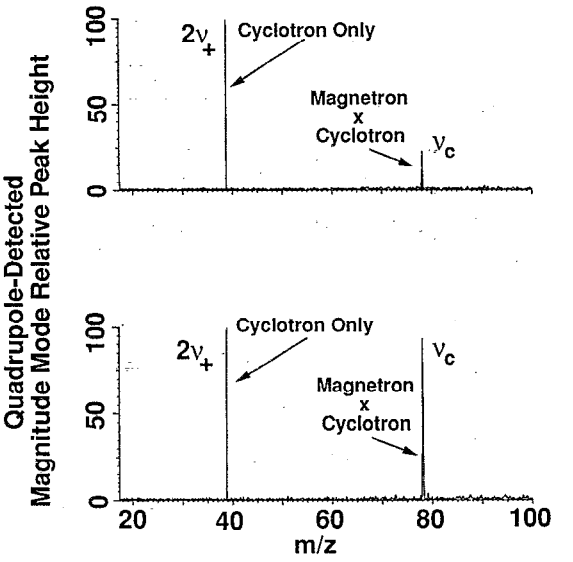

FIG. 4. FT/ICR magnitude-mode spectra (direct-mode, broad band detection to give 4 K time-domain data points, no apodization or zero-fill before FFT), obtained by quadrupolar detection following single-frequency resonant quadrupolar excitation at frequency, ν_c. Quadrupolar excitation [23.3 $V_{(p\text{-}p)}$] was applied for 0.8 ms (top, corresponding approximately to a π pulse to yield pure cyclotron motion) or 0.6 ms (bottom, to yield approximately equal ion cyclotron and magnetron radii). Note that in this detection mode, cyclotron motion is detected at frequency, $2\nu_+$, and the product of magnetron and cyclotron radii is manifested by a signal at frequency, ν_c [see Eq. (22b) and text].

cyclotron signal magnitude on prior quadrupolar excitation duration, t, and voltage, V_{xy} [see Eq. (8c)] is found by substituting Eqs. (9) and (13) into Eq. (19a),

$$|I_d(\omega_+)| = \left|\frac{q\beta}{a\omega_p}\omega_+ A_0^-\right|\left|\sin\left(\frac{\Omega_0 t}{2}\right)\right| \tag{23}$$

in which Ω_0 is given by Eq. (8c). Therefore, the signal current magnitude at frequency, ω_+, is time-modulated according to $|\sin(\Omega_0 t/2)|$ in which t is the quadrupolar excitation duration (see Fig. 3). Figure 3 shows nice agreement between experimental and theoretical [Eq. (23)] dipole-detected signal magnitude at the reduced cyclotron frequency, ω_+. For example, whenever $\Omega_0 t=(2n+1)\pi$, $n=0,1,2,...$, the magnetron motion has been completely converted to cyclotron motion, and the observed signal in Fig. 3 is maximal. Alternatively, whenever $\Omega_0 t=2n\pi$, $n=0,1,2,...$, quadrupolar excitation has driven the ions back to pure magnetron motion, and the signal in Fig. 3 is zero. Moreover, because the initial magnetron motion is coherent, the cyclotron motion obtained by magnetron-to-cyclotron conversion is also coherent and therefore detectable!

The magnetron/cyclotron interconversion process may also be monitored by observing signals at either $2\omega_+$ or ω_c in quadrupolar detection mode (see Fig. 4). The predicted signal magnitudes may be derived from Eqs. (13) and (22),

$$|I_q(2\omega_+)| = \frac{3q\alpha}{a^2}\omega_+|A_0^-|^2\left|\sin^2\left(\frac{\Omega_0 t}{2}\right)\right|$$

$$= \frac{3q\alpha}{2a^2}\omega_+|A_0^-|^2[1-\cos(\Omega_0 t)], \tag{24a}$$

$$|I_q(\omega_c)| = \frac{6q\alpha}{a^2}\omega_c|A_0^-|^2\left|\sin\left(\frac{\Omega_0 t}{2}\right)\cos\left(\frac{\Omega_0 t}{2}\right)\right|$$

$$= \frac{3q\alpha}{a^2}\omega_c|A_0^-|^2|\sin(\Omega_0 t)|. \tag{24b}$$

Note the maximum magnitude of the signal at ω_c is about twice that at $2\omega_+(\omega_+\approx\omega_c)$. The magnitude of the signal at frequency, $2\omega_+$, is time-modulated by function, $1-\cos(\Omega_0 t)$, whereas the magnitude of the signal at frequency, ω_c, is time-modulated by $|\sin(\Omega_0 t)|$. (For simplicity in display, we independently scaled the maximum signal amplitudes at ω_c and $2\omega_+$ to unity in both Figs. 5 and 6.) Figure 5 demonstrates the variation in relative signal magnitude at frequencies, $2\omega_+$, and ω_c, corresponding to interconversion between pure cyclotron and pure magnetron motion, as a function of excitation amplitude–duration product. For example, for pure cyclotron motion, $\Omega_0 t=(2n+1)\pi$, $n=0, 1, 2,...$, the quadrupole-detected signal at $2\omega_+$ is maximal [Eq. (24a)], and the quadrupole-detected signal at ω_c is zero [Eq. (24b)], as seen in Fig. 4 ($\Omega_0 t\approx\pi$, top spectrum). For pure magnetron motion, $\Omega_0 t=2n\pi$, $n=0, 1, 2,...$, the quadrupole-detected signal at $2\omega_+$ is zero [see Eq. (24a)] and the quadrupole-detected signal at ω_c is also zero [see Eq. (24b)]; the (unobserved) balance of the signal is [see Eq. (22a)] at twice the magnetron frequency, $2\omega_-$, but our detection bandwidth does not extend to that frequency.

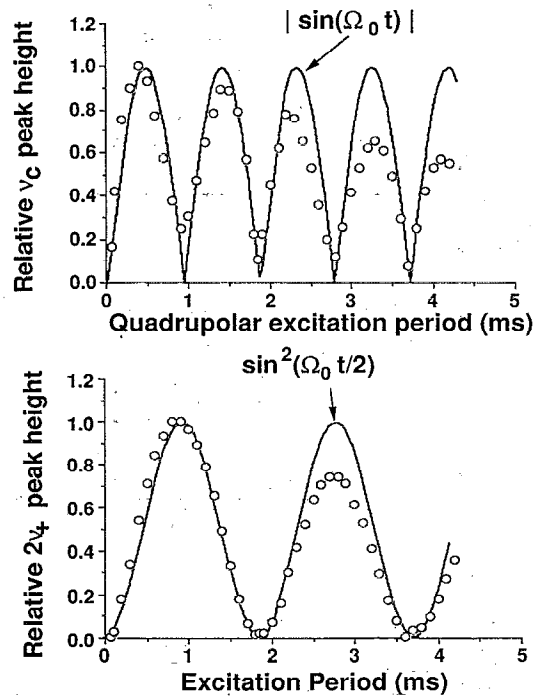

FIG. 5. Oscillation of experimental quadrupole-detected magnitude-mode (absolute-value mode) spectral peak height (open circles) at frequency, frequency, ν_c (top) or $2\nu_+$ (bottom), as a function of the duration of prior quadrupolar excitation event [12 $V_{(p\text{-}p)}$ at frequency, ν_c]. Theoretical functions, $|\sin(\Omega_0 t)|$ (top) and $\sin^2(\Omega_0 t/2)$ (bottom), based on Eqs. (24a) and (24b) are also shown as solid curves for comparison. These results clearly demonstrate the magnetron/cyclotron interconversion produced by quadrupolar excitation, e.g., note that the frequency of the sinusoid for quadrupolar detection in the top graph in this figure is twice the frequency of the otherwise similar sinusoid for dipole-detected signal in Fig. 3 [see Eqs. (23) and (24b) and accompanying text].

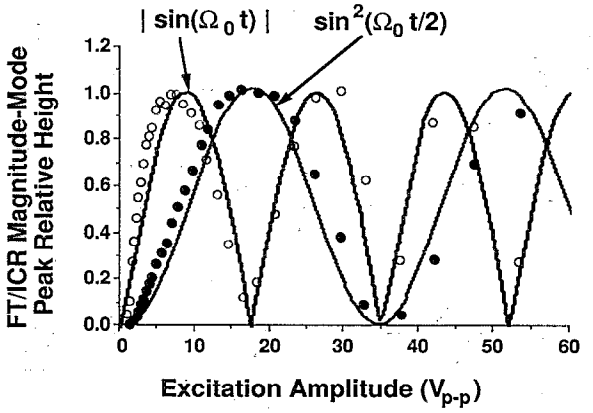

FIG. 6. Oscillation of experimental quadrupole-detected magnitude-mode (absolute-value mode) spectral peak height (open circles) at frequency, frequency, ν_c (open circles), or $2\nu_+$ (solid circles), as a function of peak-to-peak quadrupolar excitation peak-to-peak voltage (at fixed excitation duration of 0.9 ms). Theoretical functions, $|\sin(\Omega_0 t)|$ and $\sin^2(\Omega_0 t/2)$, based on Eqs. (24a) and (24b) [in which t is fixed and $V_{(p\text{-}p)}$ is varied] are also shown as solid curves for comparison. Behavior and interpretation are similar to that in Fig. 5 (see text).

Midway between pure magnetron and pure cyclotron motion, $\Omega_0 t = n\pi/2$, $n = 1, 3, 5, \ldots$, the quadrupole-detected signal at $2\omega_+$ is half the magnitude of the quadrupole-detected signal at ω_c. When $\Omega_0 t \approx 3/4$, the signal amplitudes at ω_c and $2\omega_+$ are equal to each other [see Fig. 4, bottom; we can solve for $\Omega_0 t$ by equating $1-\cos(\Omega_0 t) = 2|\sin(\Omega_0 t)|$]. Finally, note that the signal at ω_c is independent of trapping voltage (to the extent that the trapping potential is purely axially quadrupolar), for potentially improved mass accuracy.

Spectra of the type[38–40] shown in Fig. 4 were used to generate the data plotted in Figs. 5 and 6, in which quadrupole-detected magnitude-mode FT/ICR mass spectral peak height is plotted against the excitation amplitude–duration product. In Fig. 5, excitation duration is varied at constant excitation amplitude; whereas in Fig. 6, excitation amplitude is varied at constant excitation duration. As predicted by Eqs. (24), Figs. 5 and 6 show essentially the same behavior (e.g., successive minima in peak height at ω_c correspond to alternating maxima and minima in peak height at $2\omega_+$). The decrease in signal with increasing quadrupolar excitation duration in Figs. 3 and 5 presumably arises from dephasing of the ion packet during quadrupolar excitation and/or spatial nonuniformity of the quadrupolar excitation electric field. Collision-induced signal decay is probably not as significant at the pressure of 5.0×10^{-8} Torr for these experiments. There is almost no signal decay with increasing quadrupolar excitation amplitude in Fig. 6 because all of those data were obtained at the same (short) excitation duration.

B. Control of cyclotron phase coherence in a two ion packet experiment

An illuminating dividend of the present approach is that it becomes possible to observe directly the phase-coherence of ion cyclotron motion, if experiments are carried out with two off-center time-separated electron beam pulses. A first ion packet is formed by irradiation with an off-axis electron beam for a period short ($\sim$250 μs) compared to one cycle of ion magnetron motion ($\sim$4.4 ms) at 4 V trapping voltage applied to each trapping electrode). The first packet then proceeds along its magnetron orbit. A second ion packet is then produced by off-axis $\sim$250 μs electron beam irradiation. Each of the two ion packets contains the same number of ions and the same magnetron radius, but the two packets differ in magnetron phase by $\Delta\phi_-$ radians, according to the time separation, t_1, between the two electron beam events,

$$\Delta\phi_- = \phi_{2\_} - \phi_{1\_} = \omega_- t_1, \tag{25}$$

in which $\phi_{1\_}$ and $\phi_{2\_}$ are the magnetron phases of the first and the second ion packets, respectively. In the absence of excitation, the two ion packets continue to precess around the same magnetron orbit and maintain the constant phase difference, $\Delta\phi_-$. Azimuthal quadrupolar resonant excitation converts the magnetron motion of each ion packet to cyclotron motion. We may choose the quadrupolar excitation amplitude and duration such that the conversion is complete ($\Omega_0 t = \pi$), as shown in Figs. 3–6. Moreover, the magnetron-to-cyclotron conversion process is not only in-

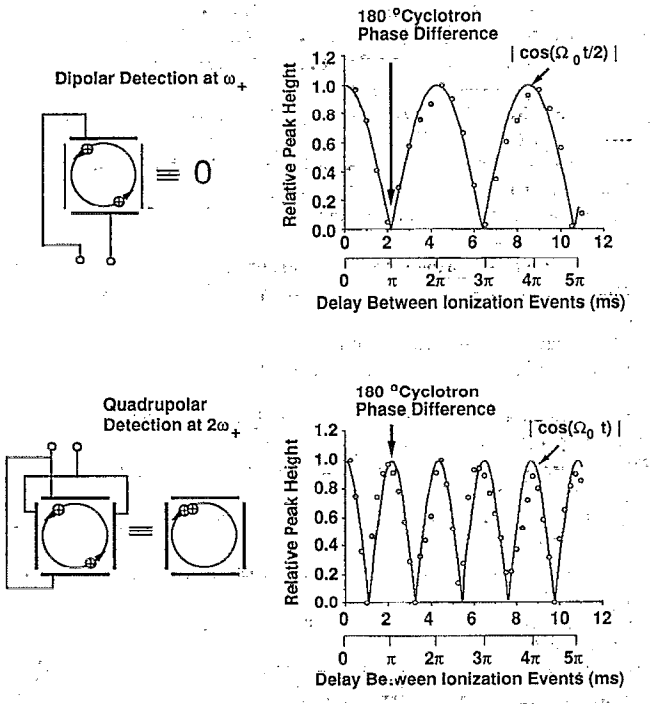

FIG. 7. Dipolar detection at frequency, ω_+ (top) and quadrupolar detection at frequency, $2\omega_+$ (bottom), following quadrupolar complete magnetron-to-cyclotron conversion of two ion packets whose initial magnetron phases are determined by the delay between the two short electron beam pulses that created the two packets. Ion packets with initial magnetron phase difference of π radians (leading to final cyclotron phase difference of π radians), give zero dipole- and maximal quadrupole-signals. Experiment data (electron beam, 500–1750 μA, −20 eV energy, and 250 μs duration), are shown as open circles, in excellent agreement with theoretical solid curves based on Eqs. (26) and (27) (see text).

dependent of the initial magnetron phase [Eq. (10a)], but the final postconversion cyclotron orbital phase is determined by the initial preconversion magnetron phase. *Thus, the postconversion cyclotron phase difference between the two ion packets is the same as the preconversion magnetron phase difference.* Because we can control the preconversion magnetron phase difference between the two ion packets simply by changing the time-delay, t_1, between the two electron beam events, we therefore now have a method for producing two ion packets rotating at the cyclotron frequency with the same cyclotron radius (equal to the preconversion magnetron radius) and controllable cyclotron phase difference.

For example, it is interesting to generate two ion packets differing by 180° in cyclotron phase. Because the ion packets have the same cyclotron radius and contain the same number of ions, there will be no net differential image charge between two opposed detection electrodes and thus no dipole-detectable signal, even at large ion cyclotron orbital radius (see Fig. 7, upper left diagram).

For dipolar detection of two cyclotron-orbiting ion packets of cyclotron phase, $\phi_{1\_}$ and $\phi_{2\_}$, the frequency-domain signal magnitude at frequency, ω_+, is just the sum of the signals from the two individual packets

$$
\begin{aligned}
|I_d(\omega_+)| &= |I_{d1}(\omega_+) + I_{d2}(\omega_+)| \\
&= \left|\frac{q\beta}{a\omega_p}\omega_+ A_0^-\right| |e^{i\phi_{1\_}} + e^{i\phi_{2\_}}| \\
&= \left|\frac{2q\beta}{a\omega_p}\omega_+ A_0^-\right| \left|\cos\left(\frac{\phi_{2\_} - \phi_{1\_}}{2}\right)\right| \\
&= \left|\frac{2q\beta}{a\omega_p}\omega_+ A_0^-\right| \left|\cos\left(\frac{\omega_- t_1}{2}\right)\right|. \qquad (26)
\end{aligned}
$$

The dipole signal magnitude oscillates sinusoidally as a function of t_1, and reaches its maximum whenever $\omega_- t_1 = 2n\pi$, $n=0, 1, 2,...$, corresponding to spatial overlap of the two ion packets. The dipole-detected signal magnitude goes to zero whenever $\omega_- t_1 = (2n+1)\pi$, $n=0, 1, 2,...$, corresponding to cyclotron phase difference of π radians for two ion packets on opposite sides of the cyclotron orbit. Our experimental results (Fig. 7, upper right) agree quite closely with the magnitude-mode relative peak height dependence on t_1 predicted by Eq. (26).

Similarly, a quadrupole-detected signal for two ion packets of equal cyclotron radius and ion number but different cyclotron phase (Fig. 7 lower left) will be observed at frequency, $2\omega_+$, with magnitude

$$
\begin{aligned}
|I_q(2\omega_+)| &= |I_{q1}(2\omega_+) + I_{q2}(2\omega_+)| \\
&= \left|\frac{3q\alpha}{a^2\omega_p^2}\omega_+ (A_0^-)^2\right| |e^{i2\phi_{1\_}} + e^{i2\phi_{2\_}}| \\
&= \left|\frac{6q\alpha}{a^2\omega_p}\omega_+ (A_0^-)^2\right| |\cos(\omega_- t_1)|. \qquad (27)
\end{aligned}
$$

Note that the quadrupole-detected signal of Eq. (27) (Fig. 7, lower left) oscillates twice as fast as a function of t_1 as the dipole-detected signal of Eq. (26) (Fig. 7, upper left). Whenever the two ion packets differ by π radians in cyclotron phase, the dipole-detected cyclotron signal is zero [Eq. (26)], whereas the quadrupole-detected signal is a maximum.

V. CONCLUSIONS

First, by forming (off-axis) ions with a nonzero initial magnetron radius, we are able to render magnetron-to-cyclotron interconversion produced by azimuthal quadrupolar excitation) observable by use of azimuthal dipolar detection at frequency, ω_+, or azimuthal quadrupolar detection at frequencies, ω_c and $2\omega_+$. It is therefore now possible to monitor the magnetron-to-cyclotron conversion process as a function of various experimental parameters (e.g., trapping potential, number of ions, ion initial displacement from the z-axis, excitation amplitude) to characterize the important new tool of quadrupolar excitation for "shrink-wrapping" an ion ensemble into a compact ion packet localized near the center of an ICR ion trap. Alternatively, the conservation of ion radius in the magnetron-to-cyclotron conversion offers a particularly direct new way to measure the number of ions in an ICR ion trap as follows. Suppose that ions are generated at a (known)

magnetron radius by off-axis ionization (as in this paper) or injection. A subsequent quadrupolar "π"-pulse will yield a packet of ions with a cyclotron radius exactly equal to the original (known) magnetron radius. The number of ions may then be obtained from the measured dipole-detected differential current between two opposed detection electrodes,[25] with the advantage that the cyclotron radius need not be determined separately from measurement of the ratio of signals at third-harmonic and fundamental cyclotron frequency.[37,45,46]

Second, by exploiting the conservation of phase in proceeding from magnetron to cyclotron motion, we are able to use a pulse–delay–pulse off-axis electron beam ionization event followed by resonant azimuthal quadrupolar excitation to produce two ion packets of equal cyclotron orbital radius and ion number but different cyclotron orbital phase. This experiment offers a direct method for study of dephasing mechanisms which reduce ion cyclotron orbital coherence.

Finally, the mass resolving power in azimuthal quadrupolar detection experiments demonstrated here can potentially increase by a factor of 2 over conventional dipole-detection, because one can observe signals at frequency, $2\omega_+$, rather than at ω_+, much as in harmonic detection experiments.[47–50]

ACKNOWLEDGMENTS

We thank Dr. L. Schweikhard for valuable discussions. This work was supported by the U.S.A. National Science Foundation (CHE-9021058), the U.S.A. Public Health Service (N.I.H. GM-31683), and The Ohio State University, and the National High Magnetic Field Laboratory at Florida State University.

[1] B. S. Freiser, Chemtracts Anal. Phys. Chem. **1**, 65 (1989).
[2] S. Ghaderi, Ceram. Trans. **5**, 73 (1989).
[3] J. R. Gord and B. S. Freiser, Anal. Chim. Acta **225**, 11 (1989).
[4] P. Sharpe and D. E. Richardson, Coord. Chem. Rev. **93**, 59 (1989).
[5] K.-P. Wanczek, Int. J. Mass Spectrom. Ion Proc. **95**, 1 (1989).
[6] C. L. Wilkins, A. K. Chowdhury, L. M. Nuwaysir, and M. L. Coates, Mass Spectrom. Rev. **8**, 67 (1989).
[7] B. S. Freiser, in *Bonding Energetics in Organometallic Compounds*, edited by T. J. Marks (American Chemical Society, Washington, D.C., 1990), Vol. 428, p. 55.
[8] D. A. Laude, Jr. and J. D. Hogan, Tech. Mess. **57**, 155 (1990).
[9] *Lasers in Mass Spectrometry*, edited by D. M. Lubman (Oxford University, New York, 1990).
[10] N. M. M. Nibbering, Acc. Chem. Res. **23**, 279 (1990).
[11] J. E. Campana, *Laser Probe Mass Spectrometry, Proc. SPIE Applied Spectroscopy in Material Science* (International Society for Optical Engineering, Bellingham, WA, 1991), Vol. 1437, p. 138.
[12] A. G. Marshall and P. B. Grosshans, Anal. Chem. **63**, 215 (1991).
[13] L. M. Nuwaysir, C. L. Wilkins, *MALD by FTMS, Proc. SPIE Applied Spectroscopy in Material Science* (International Society for Optical Engineering, Bellingham, WA, 1991), Vol. 1437, p. 112.
[14] K. Eller and H. Schwartz, Chem. Rev. **91**, 1121 (1991).
[15] R. C. Dunbar, Mass Spectrom. Rev. **11**, 309 (1992).
[16] C. B. Jacoby, C. L. Holliman, and M. L. Gross, in *Mass Spectrometry in the Biological Sciences: A Tutorial*, edited by M. L. Gross (Kluwer Academic, Dordrecht, 1992), p. 93.
[17] C. Köster, M. S. Kahr, J. A. Castoro, and C. L. Wilkins, Mass Spectrom. Rev. **11**, 495 (1992).
[18] A. G. Marshall and L. Schweikhard, Int. J. Mass Spectrom. Ion Proc. **118/119**, 37 (1992).
[19] L. Schweikhard, G. M. Alber, and A. G. Marshall, Phys. Scr. **46**, 598 (1992).
[20] J. P. Speir, G. S. Gorman, and I. J. Amster, in *Mass Spectrometry in the Biological Sciences: A Tutorial*, edited by M. L. Gross (Kluwer Academic, Dordrecht, 1992), p. 199.
[21] M. V. Buchanan and R. L. Hettich, Anal. Chem. **65**, 245 (1993).
[22] L. Schweikhard and A. G. Marshall, J. Am. Soc. Mass Spectrom. **4**, 433 (1993).
[23] L. S. Brown and G. Gabrielse, Rev. Mod. Phys. **58**, 233 (1986).
[24] M. B. Comisarow, J. Chem. Phys. **69**, 4097 (1978).
[25] P. A. Limbach, P. B. Grosshans, and A. G. Marshall, Anal. Chem. **65**, 135 (1993).
[26] M. Wang and A. G. Marshall, Int. J. Mass Spectrom. Ion Proc. **100**, 323 (1990).
[27] S. C. Beu and D. A. Laude, Jr., Int. J. Mass Spectrom. Ion Proc. **108**, 255 (1991).
[28] G. Bollen, R. B. Moore, G. Savard, and H. Stolzenberg, Appl. Phys. **68**, 4355 (1990).
[29] G. Savard, S. Becker, G. Bollen, H.-J. Kluge, R. B. Moore, L. Schweikhard, H. Stolzenberg, and U. Wiess, Phys. Lett. A **158**, 247 (1991).
[30] L. Schweikhard, S. Guan, and A. G. Marshall, Int. J. Mass Spectrom. Ion Proc. **120**, 71 (1992).
[31] S. Guan, M. C. Wahl, T. D. Wood, and A. G. Marshall, Anal. Chem. **65**, 1753 (1993).
[32] J. P. Speir, G. S. Gorman, C. C. Pitsenberger, C. A. Turner, P. P. Wang, and I. J. Amster, Anal. Chem. **65**, 1746 (1993).
[33] C. L. Hendrickson, S. A. Hofstadler, S. C. Beu, and D. A. Laude, Jr., Int. J. Mass Spectrom. Ion Proc. **123**, 49 (1993).
[34] S. Guan and A. G. Marshall, J. Chem. Phys. **98**, 4486 (1993).
[35] W. Shockley, J. Appl. Phys. **9**, 635 (1938).
[36] R. C. Dunbar, Int. J. Mass Spectrom. Ion Proc. **56**, 1 (1984).
[37] P. B. Grosshans, P. J. Shields, and A. G. Marshall, J. Chem. Phys. **94**, 5341 (1991).
[38] L. Schweikhard, Rapid Commun. Mass Spectrom. **4**, 360 (1990).
[39] L. Schweikhard, M. Lindinger, and H.-J. Kluge, Int. J. Mass Spectrom. Ion Proc. **98**, 25 (1990).
[40] L. Schweikhard, Int. J. Mass Spectrom. Ion Proc. **107**, 281 (1991).
[41] M. B. Comisarow, Int. J. Mass Spectrom. Ion Phys. **37**, 251 (1981).
[42] J. Byrne and P. S. Farago, Proc. Phys. Soc. **86**, 801 (1965).
[43] P. B. Grosshans and A. G. Marshall, Int. J. Mass Spectrom. Ion Proc. **100**, 347 (1990).
[44] R. C. Dunbar, J. H. Chen, and J. D. Hays, Int. J. Mass Spectrom. Ion Phys. **57**, 39 (1984).
[45] P. B. Grosshans, P. J. Shields, and A. G. Marshall, J. Am. Chem. Soc. **112**, 1275 (1990).
[46] P. B. Grosshans and A. G. Marshall, Int. J. Mass Spectrom. Ion Proc. **115**, 1 (1992).
[47] Y. P. Pan, D. P. Ridge, and A. L. Rockwood, Int. J. Mass Spectrom. Ion Proc. **84**, 293 (1988).
[48] E. N. Nikolaev, M. V. Gorshkov, A. V. Mordehai, and V. L. Talrose, Rapid Commun. Mass Spectrom. **4**, 144 (1990).
[49] P. B. Grosshans and A. G. Marshall, Int. J. Mass Spectrom. Ion Proc. **107**, 49 (1991).
[50] P. A. Limbach, P. B. Grosshans, and A. G. Marshall, Int. J. Mass Spectrom. Ion Proc. **123**, 41 (1993).